

Neural Enhancement of Factor Graph-based Symbol Detection

Luca Schmid and Laurent Schmalen

Communications Engineering Lab (CEL), Karlsruhe Institute of Technology (KIT)
Hertzstr. 16, 76187 Karlsruhe, Germany, Email: {first.last}@kit.edu

Abstract—We study the application of the factor graph framework for symbol detection on linear inter-symbol interference channels. Cyclic factor graphs have the potential to yield low-complexity symbol detectors, but are suboptimal if the ubiquitous sum-product algorithm is applied. In this paper, we present and evaluate strategies to improve the performance of cyclic factor graph-based symbol detection algorithms by means of neural enhancement. In particular, we apply neural belief propagation as an effective way to counteract the effect of cycles within the factor graph. We further propose the application and optimization of a linear preprocessor of the channel output. By modifying the observation model, the preprocessing can effectively change the underlying factor graph, thereby significantly improving the detection performance as well as reducing the complexity.

Index Terms—Factor graphs, neural belief propagation, symbol detection, channels with memory

I. INTRODUCTION

Factor graphs are a flexible tool for algorithmic modeling of efficient inference algorithms. By representing the factorization of a composite global function of many variables in a graphical way, the computation of various marginalizations of this function can be efficiently implemented by a message passing algorithm. That is why many well-known algorithms like the Viterbi algorithm, the BCJR algorithm or Pearl’s belief propagation can be derived by message passing on a suitable factor graph [1]. While being originally derived for tree-structured graphs, message passing schemes, like the sum-product algorithm (SPA), can also be applied to cyclic graphs, which leads to iterative, suboptimal algorithms.

In this paper, we investigate the behavior of the SPA on cyclic factor graphs for the well-known task of a transmission over an additive white Gaussian noise (AWGN) channel affected by linear inter-symbol interference (ISI). Modeling a factor graph based on the *Forney* observation model [2] leads to a detection algorithm with a complexity that is linear in the block length but exponential in the number of interferers [3]. Alternatively, the symbol detector in [4] employs a factor graph based on the *Ungerboeck* observation model [5] and has significantly reduced complexity. However, both algorithms show a greatly differing performance and the low-complexity detector may suffer from large performance penalties.

Recently, model-based deep learning has shown great potential to empower various communication algorithms [6] and

overcome their limitations. In [7], the factor nodes (FNs) of a cycle-free factor graph are replaced by deep neural networks (DNNs) that are utilized to learn the local mappings of the FNs, thereby robustifying the algorithm towards model uncertainties. To mitigate the performance loss for cyclic factor graphs, a graph neural network (GNN), which is structurally identical to the original graph, but has fully parametrized message updates is used in [8]. The GNN runs conjointly to the original algorithm and corrects the SPA messages after each iteration. The authors in [9] compensate the performance degradation due to cycles in the graph by concatenating a supplemental neural network (NN)-based FN to the factor graph. This additional FN is connected to all variable nodes (VNs) and is optimized in an end-to-end manner. However, the underlying NN structure is specifically tailored to binary transmission which substantially limits its scope of application.

Instead of replacing different components of the factor graph by DNNs, the SPA is unfolded to a DNN and the resulting graph is equipped with tunable weights in [10]. This approach is known as neural belief propagation (NBP). In this paper, we consider NBP for the application of factor graph-based symbol detection. Since the performance improvement of NBP is limited, we propose a novel generalization of the factor graph by introducing additional multiplicative weights within the FNs. Optimizing all weights in an end-to-end manner already leads to considerable performance gains. Moreover, we leverage the high sensibility of the SPA to a variation of the underlying graph structure by applying an optimizable linear filter to the channel output, which allows us to modify the observation model and thereby the factor graph itself. Varying the filter order, the proposed generalization provides an adjustable performance-complexity tradeoff and can significantly outperform conventional factor graph models, which we illustrate by simulations for two different ISI channels and two different modulation formats.

II. FACTOR GRAPHS AND MARGINALIZATION

Let $f(\mathcal{X})$ be a multivariate function which depends on the set of variables $\mathcal{X} = \{x_0, \dots, x_n\}$ and which can be factorized as

$$f(\mathcal{X}) = \prod_{j=1}^J f_j(\mathcal{X}_j), \quad \mathcal{X}_j \subset \mathcal{X}. \quad (1)$$

A *factor graph* represents the factorization of $f(\mathcal{X})$ in a graphical way [1]. The following rules define the bijective relationship between (1) and its corresponding factor graph:

This work has received funding in part from the European Research Council (ERC) under the European Union’s Horizon 2020 research and innovation programme (grant agreement No. 101001899) and in part from the German Federal Ministry of Education and Research (BMBF) within the project Open6GHub (grant agreement 16KISK010).

- Every factor $f_j(\mathcal{X}_j)$ is represented by a unique vertex, the so-called FN f_j .
- Every variable $x \in \mathcal{X}$ is represented by a unique vertex, the so-called VN x .
- An FN f_j is connected to a VN x if and only if the corresponding factor $f_j(\mathcal{X}_j)$ is a function of x , i.e., if $x \in \mathcal{X}_j =: \mathcal{N}(f_j)$.

The notation $\mathcal{N}(f_j)$ is called the *neighborhood* of the FN f_j . Equivalently, $\mathcal{N}(x) := \{f_j : x \in \mathcal{X}_j, j = 1, \dots, J\}$ denotes the neighborhood of the VN x .

The SPA is a message passing algorithm which computes the marginalization $f(x_i)$ of the global function $f(\mathcal{X})$ with respect to each variable $x_i \in \mathcal{X}$, respectively. By operating on a factor graph, it implicitly leverages the distributive law on the factorization of $f(\mathcal{X})$. Messages are propagated between the nodes of the factor graph along its edges and represent interim results of the marginalization. Let $\mu_{f_j \rightarrow x}(x)$ denote a message sent from FN f_j along an edge to VN x . Consequently, $\mu_{x \rightarrow f_j}(x)$ denotes a message on the same edge, but sent in the opposite direction. The message passing algorithm is based on one central message update rule for the FNs and VNs, respectively. In the logarithmic domain, the message updates are

$$\mu_{x \rightarrow f_j}(x) = \sum_{f' \in \mathcal{N}(x) \setminus \{f_j\}} \mu_{f' \rightarrow x}(x) \quad (2)$$

$$\mu_{f_j \rightarrow x}(x) = \max_{\sim \{x\}}^* \left(\ln(f_j(\mathcal{X}_j)) + \sum_{x' \in \mathcal{N}(f_j) \setminus \{x\}} \mu_{x' \rightarrow f_j}(x') \right). \quad (3)$$

The operator $\max_{\sim \{x\}}^* \delta_i$ denotes the Jacobian logarithm [11] which computes $\ln(e^{\delta_1} + \dots + e^{\delta_n})$. Applying the Jacobian logarithm over all variables of a function except x is denoted by the *summary* operator $\max_{\sim \{x\}}^*$. Based on the SPA message update rule, we can compute marginals by propagating messages through the respective factor graph. If the graph is tree-structured, messages travel forward and backward through the entire graph, starting at the leaf nodes. Based on the computed messages, the exact marginals

$$f(x_i) = \exp \left(\sum_{f' \in \mathcal{N}(x_i)} \mu_{f' \rightarrow x_i}(x_i) \right), \quad x_i \in \mathcal{X} \quad (4)$$

can be obtained. Since the message updates are local [1] and because the SPA makes no reference to the topology of the graph [12], the SPA may also be applied to factor graphs with cycles, yielding an iterative algorithm. The messages are initialized with an unbiased state in iteration $n = 0$ and are iteratively updated by following a certain schedule until convergence or a stopping criterion is reached. In the case of cyclic factor graphs, the superscript (n) , with $n = 0, \dots, N$ indicates the iteration in which the message $\mu_{a \rightarrow b}^{(n)}$ is computed. In contrast to tree-structured graphs, this iterative algorithm only yields an approximation of the exact marginals [1]. However, many successful applications, e.g., decoders of error-correcting codes, are based on message passing on cyclic graphs [12].

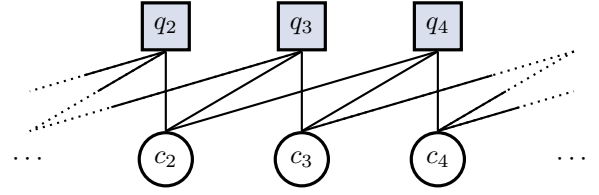


Fig. 1: Factor graph representation of (8) for $L = 2$.

III. SYMBOL DETECTION

We consider the transmission of an information sequence $\mathbf{c} \in \mathcal{M}^K$ of a multilevel constellation $\mathcal{M} = \{m_i \in \mathbb{C}, i = 1, \dots, M\}$ over a baseband channel, impaired by linear intersymbol interference and AWGN. The bit pattern of length $m := \log_2(M)$ which corresponds to a symbol c_k is denoted by $\mathbf{b}(c_k) = (b_1(c_k), \dots, b_m(c_k))$. The relationship between the independent and uniformly distributed symbols c_k and the receive symbols y_k can be expressed by an equivalent discrete-time channel model [2]:

$$y_k = \sum_{\ell=0}^L h_\ell c_{k-\ell} + w_k, \quad k = 1, \dots, K+L. \quad (5)$$

For a channel with memory L , $\mathbf{h} \in \mathbb{C}^{L+1}$ is the finite channel impulse response and $\mathbf{w} \sim \mathcal{CN}(0, \sigma^2 \mathbf{I})$ denotes white circular Gaussian noise. We assume that the symbols c_k for $k \leq 1$ and $k > K$ represent the known initial state and the steady state of the channel filter. Since the interference is linear, (5) can be described in matrix vector notation

$$\mathbf{y} = \mathbf{H}\tilde{\mathbf{c}} + \mathbf{w}, \quad \mathbf{H} \in \mathbb{C}^{(K+L) \times (K+2L)}$$

with the equivalent transmit sequence $\tilde{\mathbf{c}} := (c_{1-L}, \dots, c_{K+L})$.

We study the problem of symbol detection, i.e., the estimation of the symbols c_k from the observed sequence \mathbf{y} . In the context of Bayesian inference, we are interested in the symbol-wise a posteriori probabilities (APPs)

$$P(c_k = m | \mathbf{y}) = \sum_{\mathbf{c} \in \mathcal{M}^K, c_k = m} P(\mathbf{c} | \mathbf{y}), \quad k = 1, \dots, K. \quad (6)$$

The marginalization in (6) can be efficiently computed by the SPA if the APP distribution $P(\mathbf{c} | \mathbf{y})$ can be represented by a suitable factor graph. Applying Bayes' theorem and exploiting the uniform distribution of the independent information symbols, we obtain

$$P(\mathbf{c} | \mathbf{y}) \propto p(\mathbf{y} | \mathbf{c}) = \frac{1}{(\pi\sigma^2)^K} \exp \left(-\frac{\|\mathbf{y} - \mathbf{H}\mathbf{c}\|^2}{\sigma^2} \right). \quad (7)$$

Using the chain rule of conditional probabilities and exploiting the Markovian property of the channel with finite memory L and AWGN, we factorize the likelihood function

$$\begin{aligned} p(\mathbf{y} | \mathbf{c}) &\propto \prod_{k=1}^K \exp \left(-\frac{|y_k - \sum_{\ell=0}^L h_\ell c_{k-\ell}|^2}{\sigma^2} \right) \\ &=: \prod_{k=1}^K q_k(c_k, c_{k-1}, \dots, c_{k-L}) \end{aligned} \quad (8)$$

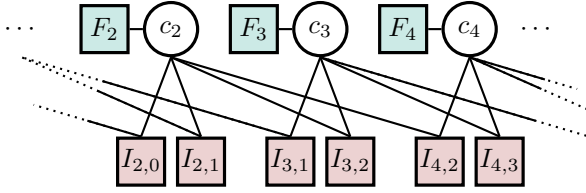


Fig. 2: Factor graph representation of (10) for $L = 2$.

and represent it by a factor graph, as illustrated in Fig. 1. By running the SPA on this factor graph, we obtain a symbol detection algorithm that we call FFG (Forney-based factor graph symbol detector) and which was initially proposed in [3]. Alternatively, we can rewrite the exponential term in (7) as

$$p(\mathbf{y}|\mathbf{c}) \propto \exp\left(\frac{2\text{Re}\{\mathbf{c}^H \mathbf{H}^H \mathbf{y}\} - \mathbf{c}^H \mathbf{H}^H \mathbf{H} \mathbf{c}}{\sigma^2}\right),$$

where proportionality \propto denotes two terms only differing in a factor independent of \mathbf{c} . By substituting

$$\mathbf{G} := \mathbf{H}^H \mathbf{H}, \quad \mathbf{x} := \mathbf{H}^H \mathbf{y}, \quad (9)$$

and using the scalar notation

$$\begin{aligned} \mathbf{c}^H \mathbf{x} &= \sum_{k=1}^K x_k c_k^* \\ \mathbf{c}^H \mathbf{G} \mathbf{c} &= \sum_{k=1}^K G_{k,k} |c_k|^2 - \sum_{k=1}^K \sum_{\substack{\ell=1 \\ \ell \neq k}}^K \text{Re}\{G_{k,\ell} c_\ell c_k^*\}, \end{aligned}$$

an alternative factorization

$$p(\mathbf{y}|\mathbf{c}) \propto \prod_{k=1}^K \left[F_k(c_k) \prod_{\substack{\ell=1 \\ \ell \neq k}}^K J_{k,\ell}(c_k, c_\ell) \right] \quad (10)$$

with the factors

$$F_k(c_k) := \exp\left(\frac{1}{\sigma^2} \text{Re}\{2x_k c_k^* - G_{k,k} |c_k|^2\}\right) \quad (11)$$

$$J_{k,\ell}(c_k, c_\ell) := \exp\left(-\frac{1}{\sigma^2} \text{Re}\{G_{k,\ell} c_\ell c_k^*\}\right) \quad (12)$$

can be found [4]. Figure 2 illustrates the factor graph corresponding to (10). The factors $J_{k,\ell}(c_k, c_\ell)$ and $J_{\ell,k}(c_\ell, c_k)$ depend on the same variables and can be condensed to one factor $I_{k,\ell}(c_k, c_\ell) := J_{k,\ell}(c_k, c_\ell) J_{\ell,k}(c_\ell, c_k)$ with $k > \ell$. Applying the SPA on the factor graph in Figure 2 yields an alternative symbol detection algorithm which we call UFG (Ungerboeck-based factor graph symbol detector). It was initially proposed by Colavolpe in [4].

For both FFG and UFG algorithms, all messages are initialized with $\mu_0(c_k) := -\ln(M)$ and we perform N SPA iterations. We apply a flooding schedule, i.e., one iteration comprises the simultaneous update of all messages from VNs to FNs in a first step, followed by the update of messages propagating in the opposite direction in a second step. The soft output $\hat{P}(c_k|\mathbf{y})$ is finally obtained by applying (4) to all VNs.

Although the factorizations (8) and (10) are both exact, the FFG and UFG algorithms are both suboptimal due to cycles within the underlying graphs and only yield an approximation for the symbol-wise APPs.

The complexity of factor graph-based algorithms can be estimated by the number of message updates at the FNs, since the FN update rule (3) is computationally more demanding than the operation (2) at the VNs. The asymptotic complexity of the FFG algorithm is $\mathcal{O}(NKLM^L)$ [3]. In contrast, the UFG algorithm has a significantly reduced complexity in the order of $\mathcal{O}(NKLM^2)$ which only grows linearly with both the block length K and the channel memory L [4].

IV. NEURAL BELIEF PROPAGATION ON FACTOR GRAPHS

By the use of deep unfolding, first introduced in [13], an iterative algorithm can be converted into a DNN. Unfolding the N SPA iterations on a factor graph is natural since each iteration is already (factor) graph-based. The resulting unrolled DNN comprises N layers and messages are propagated in a feed-forward fashion through the layers of the network. VNs and FNs accept incoming messages from the previous layer and apply the SPA message update rule. The resulting outgoing messages are then forwarded downstream to the next layer. As a consequence, each transmitted message in every iteration has its individually assigned edge. By accordingly weighting each message per edge, we attempt to mitigate the effects of short cycles and improve the performance of message passing on cyclic factor graphs. Optimizing the weights towards a loss function by the use of established deep learning techniques is known as NBP [10]. In consistency with the message notation, the message $\mu_{x \rightarrow f}^{(n)}(x)$ is multiplied by the weight $w_{x \rightarrow f}^{(n)}$. We parametrize the NBP of the FFG and UFG algorithms by

$$\mathcal{P}_{\text{FFG}} := \{w_{p_k \rightarrow c_{k-\ell}}^{(n)}, w_{c_{k-\ell} \rightarrow p_k}^{(n)}, \ell = 0, \dots, L, \\ n = 1 \dots, N, k = 1 \dots, K+L\},$$

and

$$\mathcal{P}_{\text{UFG}}(L) := \{w_{c_k \rightarrow I_{k,\ell}}^{(n)}, w_{I_{k,\ell} \rightarrow c_k}^{(n)}, n = 1, \dots, N, \\ k = 1, \dots, K+L, |k - \ell| = 1, \dots, L\}.$$

The FNs F_k have degree 1. Incident edges are thus not included in the cycles of the factor graph and are consequently not weighted. The computational complexity of NBP is slightly increased compared to the SPA. M additional multiplications per message are required.

The UFG algorithm can be further generalized by varying the observation model on which the factor graph is based. The original factorization in (9) implicitly uses a preprocessor by applying a matched filter $\mathbf{P} = \mathbf{H}^H$ to the channel observation \mathbf{y} . Inference is carried out using the new observation \mathbf{x} , based on the so called Ungerboeck observation model [5] which is characterized by \mathbf{G} and directly affects the underlying factor graph in (11) and (12). We generalize the preprocessor to a generic finite impulse response (FIR) filter by modifying the observation model to

$$\tilde{\mathbf{G}} := \mathbf{P} \mathbf{H}, \quad \tilde{\mathbf{x}} := \mathbf{P} \mathbf{y},$$

where \mathbf{P} is a convolutional Toeplitz matrix based on the generic impulse response $\mathbf{p} \in \mathbb{R}^{L_p}$ of an FIR preprocessing filter. Applying the SPA on this modified factor graph yields a novel detection algorithm which we call GFG(\mathbf{P}). The instance GFG(\mathbf{H}^H) is equivalent to the UFG equalizer. Additionally, we generalize the FNs of the GFG algorithm by the application of multiplicative weights $\kappa_{i,k}^{(n)}$ and $\lambda_{k,\ell}^{(n)}$ in order to increase the parameter optimization space further. The resulting factors, given in the logarithmic domain, are

$$\begin{aligned}\tilde{F}_k^{(n)}(c_k) &:= \frac{\kappa_{1,k}^{(n)}}{\sigma^2} \operatorname{Re} \left\{ \kappa_{2,k}^{(n)} 2\tilde{x}_k c_k^* - \kappa_{3,k}^{(n)} \tilde{G}_{k,k} |c_k|^2 \right\} \\ \tilde{I}_{k,\ell}^{(n)}(c_k, c_\ell) &:= \lambda_{k,\ell}^{(n)} \left(\tilde{J}_{k,\ell}(c_k, c_\ell) + \tilde{J}_{\ell,k}(c_\ell, c_k) \right) \\ \tilde{J}_{k,\ell}(c_k, c_\ell) &:= -\frac{1}{\sigma^2} \operatorname{Re} \left\{ \tilde{G}_{k,\ell} c_\ell c_k^* \right\}.\end{aligned}$$

Together with the NBP weights, the set of optimizable parameters for the GFG(\mathbf{P}) algorithm is

$$\begin{aligned}\mathcal{P}_{\text{GFG}}(L_p) &:= \left\{ \mathbf{p} \in \mathbb{R}^{L_p}, \kappa_{i,k}^{(n)}, \lambda_{k,\ell}^{(n)}, k = 1, \dots, K+L, \right. \\ &\quad \left. k - \ell = 1, \dots, L, i = 1, 2, 3 \right\} \cup \mathcal{P}_{\text{UFG}}(L_p).\end{aligned}$$

A. Parameter Optimization

We optimize the parameter sets \mathcal{P}_{FFG} , \mathcal{P}_{UFG} and \mathcal{P}_{GFG} of the proposed symbol detectors towards an objective function in an end-to-end manner. Since the factor graph-based algorithms embody DNNs, we rely on a rich pool of advanced optimization and training methods developed for feed-forward DNNs in the last years. We employ the Adam algorithm [14] as a stochastic gradient descent optimizer. The gradients can be computed using backpropagation [15], which is a standard method for DNNs. All weights are initialized with 1.0 and the initial filter taps \mathbf{p} of the GFG algorithm are independently sampled from a standard normal distribution.

We optimize the parametrization towards a maximum achievable rate between the channel input and the detector output. Many practical transmission systems use bit-interleaved coded modulation (BICM), which decouples the symbol detection from a binary soft-decision forward error correction (FEC) [16]. In BICM, the symbol detector soft output $\hat{P}(c_k | \mathbf{y})$ is converted by a bit-metric decoder (BMD) to binary soft information

$$\hat{P}(b_i(c_k) = \mathbf{b} | \mathbf{y}) = \sum_{\mathbf{m} \in \mathcal{M}_i^{(\mathbf{b})}} \hat{P}(c_k = \mathbf{m} | \mathbf{y}), \quad \mathbf{b} \in \{0, 1\}$$

with $\mathcal{M}_i^{(\mathbf{b})} := \{\mathbf{m} \in \mathcal{M} : b_i(\mathbf{m}) = \mathbf{b}\}$. The resulting bit-wise APPs are typically expressed in log-likelihood ratios (LLRs)

$$L_{k,i}(\mathbf{y}) := \ln \left(\frac{\hat{P}(b_i(c_k) = 0 | \mathbf{y})}{\hat{P}(b_i(c_k) = 1 | \mathbf{y})} \right).$$

After interleaving, the LLRs are fed to a bit-wise soft-decision FEC. By interpreting the BMD as a mismatched detector, the bitwise mutual information (BMI) is an achievable information rate for BICM [16]. The calculation of the BMI, detailed

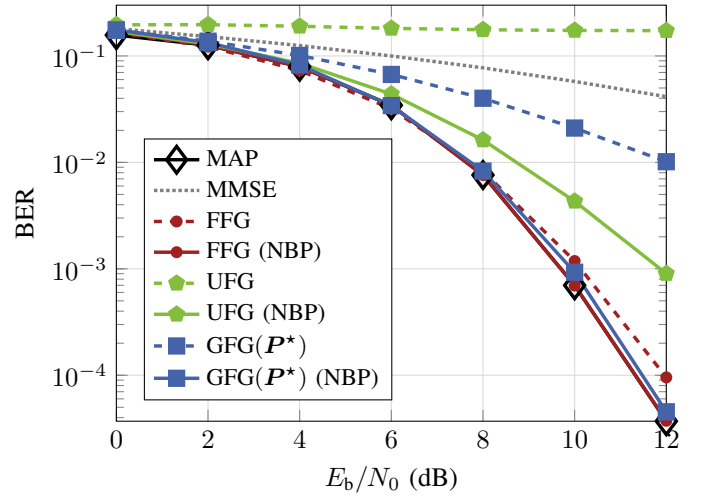


Fig. 3: BER over E_b/N_0 on the Proakis B channel with BPSK signaling for different symbol detection schemes.

in [17], considers the BMD by assuming m parallel sub-channels transmitting on a binary basis instead of one symbol-based channel. Assuming independent transmit bits, the BMI is defined as the sum of mutual informations¹ $I(b_i; y)$ of m unconditional bit-wise channel transmissions:

$$\text{BMI} := \sum_{i=1}^m I(b_i(c_k); y).$$

By a sample mean estimation over D labeled data batches $\mathcal{D} := \{(\mathbf{c}^{(d)}, \mathbf{y}^{(d)})_i : \mathbf{c}^{(d)} \in \mathcal{M}^K, \mathbf{y}^{(d)} = \mathbf{H}\mathbf{c}^{(d)} + \mathbf{w}_i, i = 1, \dots, D\}$, a feasible approximation

$$\begin{aligned}\text{BMI} &\approx \log_2(M) - \\ &\quad \frac{1}{DK} \sum_{i=1}^m \sum_{k=0}^{K-1} \sum_{(\mathbf{c}^{(d)}, \mathbf{y}^{(d)}) \in \mathcal{D}} \log_2 \left(\exp \left(-(-1)^{b_{k,i}(c_k^{(d)})} L_{k,i}(\mathbf{y}) \right) + 1 \right)\end{aligned}\quad (13)$$

can be found [17]. For gradient descent optimization, we maximize the objective function in (13).

V. NUMERICAL RESULTS

We evaluate the considered algorithms towards their detection performance. In this paper, we show the bit error rate (BER) results, however, an evaluation with respect to the BMI shows a qualitatively similar behavior. A linear minimum mean squared error (MMSE) equalizer [18, Sec. 9.4] with filter order 30 as well as the symbol-wise maximum a posteriori (MAP) detector, implemented using the BCJR algorithm [19], serve as references. We consider a block length of $K = 500$ symbols and a transmission over two standard ISI channel models: the channel *Proakis A* with an impulse response $\mathbf{h}_A := (0.04, -0.05, 0.07, -0.21, -0.5, 0.72, 0.36, 0.0, 0.21, 0.03, 0.07)^T$ and the channel *Proakis B* with $\mathbf{h}_B := (0.407, 0.815, 0.407)^T$.

Figure 3 shows the BER performance of the considered algorithms as a function of $E_b/N_0 := (m\sigma^2)^{-1}$ for a binary

¹The mutual information is a measure between two random variables. We avoid a distinct notation for random variables as it is clear from the context.

phase-shift keying (BPSK) transmission over the Proakis B channel. While the performance of the FFG detector is already close to optimal MAP detection, the UFG algorithm performs very poorly. Notably, the BER does not decrease for an increasing E_b/N_0 . We apply NBP for both detection schemes and optimize \mathcal{P}_{FFG} and \mathcal{P}_{UFG} for $E_b/N_0 = 10$ dB. Both algorithms show a performance improvement over the complete E_b/N_0 range. The optimized FFG detector approaches optimal MAP performance and the UFG algorithm shows a significant BER improvement: the application of NBP reduces the BER by a factor of more than 100 for $E_b/N_0 = 12$ dB.

We further examine the impact of the observation model on the UFG algorithm. Therefore, we generalize the pre-processing of the $\text{UFG} = \text{GFG}(\mathbf{P} = \mathbf{H}^H)$ algorithm to a generic preprocessor \mathbf{P}^* with $L_p = 7$, which we optimize with respect to the BMI for $E_b/N_0 = 10$ dB. The $\text{GFG}(\mathbf{P}^*)$ equalizer reaches a BER of 10^{-2} at $E_b/N_0 = 12$ dB, thereby outperforming the MMSE reference. By applying NBP on this modified factor graph, we achieve a detection performance which is close to optimum.

The detection performance on the Proakis A channel is evaluated in Fig. 4. For BPSK signalling, the UFG algorithm shows already a quasi-optimum performance, whereas the FFG detector has a loss of 1 dB at $E_b/N_0 = 10^{-5}$. The application of NBP improves the detection performance, but cannot entirely close the gap to the MAP performance. For 16-quadrature amplitude modulation (QAM), the FFG and the BCJR algorithm become computationally infeasible. The UFG algorithm outperforms the MMSE algorithm in the low E_b/N_0 regime but runs into an error floor. Optimizing the UFG detector for $E_b/N_0 = 14$ dB compensates this behavior and generalizes well over the complete E_b/N_0 range. The GFG algorithm with $L_p \geq L = 10$ yields similar results (not shown here to keep the figure simple).

VI. CONCLUSION

We considered the application and neural enhancement of message passing on cyclic factor graphs for symbol detection on inter-symbol interference channels. Performance and computational complexity of the algorithms strongly depend on the underlying factor graph, which can be actively varied by a change in the observation model. We proposed simple but effective generalizations of the factor graph, as well as NBP—as an enhanced message passing algorithm—in order to mitigate the effect of cycles in the graphs. The methods are only marginally increasing the detection complexity. Our numerical evaluations demonstrate the effectiveness of the proposed methods by reaching near-MAP performance for two exemplary channel models. Especially for high-order constellations and static channels with large memory, the proposed novel GFG algorithm is a promising low-complexity alternative to the BCJR.

REFERENCES

[1] F. R. Kschischang and H.-A. Loeliger, “Factor graphs and the sum-product algorithm,” *IEEE Trans. Inf. Theory*, vol. 47, no. 2, p. 22, 2001.

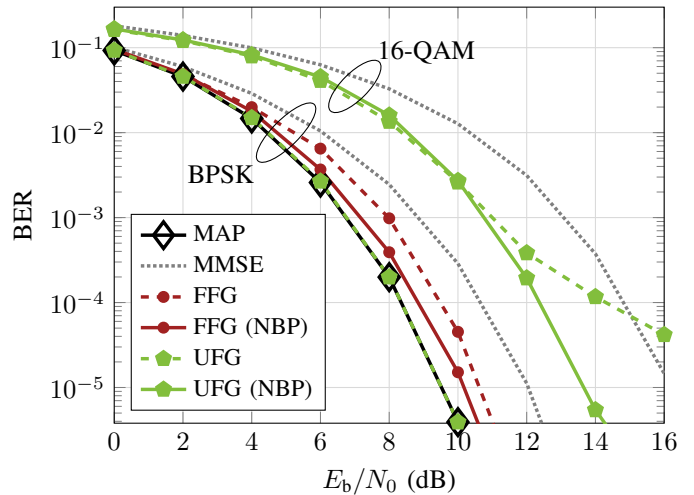


Fig. 4: Hard-decision performance of different symbol detectors for a BPSK and a 16-QAM transmission over the Proakis A channel.

[2] G. D. Forney, “Lower bounds on error probability in the presence of large intersymbol interference,” *IEEE Trans. Commun.*, Feb. 1972.

[3] G. Colavolpe and G. Geremi, “On the application of factor graphs and the sum-product algorithm to ISI channels,” *IEEE Trans. Commun.*, vol. 53, no. 5, pp. 818–825, May 2005.

[4] G. Colavolpe, D. Fertonani, and A. Piemontese, “SISO detection over linear channels with linear complexity in the number of interferers,” *IEEE J. Sel. Topics Signal Process.*, vol. 5, no. 8, Dec. 2011.

[5] G. Ungerboeck, “Adaptive maximum-likelihood receiver for carrier-modulated data-transmission systems,” *IEEE Trans. Commun.*, 1974.

[6] N. Shlezinger, J. Whang, Y. C. Eldar, and A. G. Dimakis, “Model-based deep learning,” *arXiv preprint arXiv:2012.08405*, Dec. 2020.

[7] N. Shlezinger, N. Farsad, Y. Eldar, and A. Goldsmith, “Learned factor graphs for inference from stationary time sequences,” *IEEE Trans. Signal Process.*, vol. 70, pp. 366–380, 2021.

[8] V. G. Satorras and M. Welling, “Neural enhanced belief propagation on factor graphs,” in *Proc. Int. Conf. on Artificial Intelligence and Statistics (AISTATS)*, vol. 2021, San Diego, CA, USA, 2021, pp. 685 – 693.

[9] B. Liu, S. Li, Y. Xie, and J. Yuan, “A novel sum-product detection algorithm for faster-than-Nyquist signaling: A deep learning approach,” *IEEE Trans. Commun.*, vol. 69, no. 9, pp. 5975–5987, Sep. 2021.

[10] E. Nachmani, Y. Be’ery, and D. Burshtein, “Learning to decode linear codes using deep learning,” in *Proc. Allerton Conf. on Communication, Control, and Computing*, Monticello, IL, Sep. 2016.

[11] P. Robertson, E. Villebrun, and P. Hoeher, “A comparison of optimal and sub-optimal MAP decoding algorithms operating in the log domain,” in *Proc. IEEE Int. Conf. on Communications (ICC)*, Jun. 1995.

[12] J. Yedidia, W. Freeman, and Y. Weiss, “Understanding belief propagation and its generalizations,” in *Exploring Artificial Intelligence in the New Millennium*, Jan. 2003, vol. 8, pp. 239–269.

[13] K. Gregor and Y. LeCun, “Learning fast approximations of sparse coding,” in *Proc. Int. Conf. on Machine Learning (ICML)*, Madison, WI, USA, Jun. 2010.

[14] D. P. Kingma and J. Ba, “Adam: A method for stochastic optimization,” in *Proc. Int. Conf. Learning Representations (ICLR)*, San Diego, CA, USA, May 2015.

[15] D. E. Rumelhart, G. E. Hinton, and R. J. Williams, “Learning representations by back-propagating errors,” *Nature*, vol. 323, Oct. 1986.

[16] A. Guillén i Fàbregas, A. Martinez, and G. Caire, “Bit-interleaved coded modulation,” in *Foundations and Trends in Communications and Information Theory*. Delft, NL: Now Publishers, 2008, vol. 5.

[17] A. Alvarado, T. Fehenberger, B. Chen, and F. M. J. Willems, “Achievable information rates for fiber optics: Applications and computations,” *J. Lightw. Technol.*, vol. 36, no. 2, pp. 424–439, Jan. 2018.

[18] J. Proakis and M. Salehi, *Digital Communications*, 5th ed. McGraw Hill, Nov. 2007.

[19] L. Bahl, J. Cocke, F. Jelinek, and J. Raviv, “Optimal decoding of linear codes for minimizing symbol error rate (Corresp.),” *IEEE Trans. Inf. Theory*, vol. 20, no. 2, pp. 284–287, Mar. 1974.